

Adriano Luiz de Paula*
Institute of Aeronautics and Space
São José dos Campos, Brazil
adrianoalp@iae.cta.br

Mirabel Cerqueira Rezende
Institute of Aeronautics and Space
São José dos Campos, Brazil
mirabelmcr@iae.cta.br

Joaquim José Barroso
National Institute for Space Research
São José dos Campos, Brazil
barroso@plasma.inpe.br

*author for correspondence

Experimental measurements and numerical simulation of permittivity and permeability of Teflon in X band

Abstract: Recognizing the importance of an adequate characterization of radar absorbing materials, and consequently their development, the present study aims to contribute for the establishment and validation of experimental determination and numerical simulation of electromagnetic materials complex permittivity and permeability, using a Teflon® sample. The present paper branches out into two related topics. The first one is concerned about the implementation of a computational modeling to predict the behavior of electromagnetic materials in confined environment by using electromagnetic three-dimensional simulation. The second topic re-examines the Nicolson-Ross-Weir mathematical model to retrieve the constitutive parameters (complex permittivity and permeability) of a homogeneous sample (Teflon®), from scattering coefficient measurements. The experimental and simulated results show a good convergence that guarantees the application of the used methodologies for the characterization of different radar absorbing materials samples.

Keywords: Electric permittivity, Magnetic permeability, Radar absorbing material, Computational modeling.

INTRODUCTION

Knowledge of complex permittivity, ϵ^* , and permeability, μ^* , of materials proves to be of great interest in scientific and industrial applications. The measurement of ϵ^* and μ^* in the microwave frequency range finds direct application in different areas. The electromagnetic radiation effects on biological systems study in ceramic sintering, plastic welding, and remote sensing (Chung, 2007) can be mentioned as examples. In this latter case, a good understanding of the vegetation dielectric properties is vital to get useful information from the remotely sensed data for earth resources monitoring and management, because the vegetation dielectric constant has a direct effect on radar backscattering measured by microwave sensors. Concerning sectors of electronic, telecommunication, aerospace industries, and in particular in the research and development of radar absorbing materials (RAM), the knowledge of ϵ^* and μ^* allows to predict the electromagnetic properties of materials via computer simulation. Thus, the simulation is useful for supporting studies related to the RAM processing optimization, as well as its utilization for specific purposes.

Computational modeling becomes relevant as long as the simulated results reproduce and anticipate experimentally

measured data. Strong interrelation between modeling and experimental contributes to ensure confidence in the computational tool developed for a given application. A purpose of computer modeling is to reconstruct experimental measurements aiming at understanding and evaluating measured parameters, and also to obtain new parameters in different contexts but consistent with the experimental interpretation. In situations in which a modal analysis turns out too complex and difficult to solve, numerical methods are widely used, such as finite element method (FEM), finite difference method (FDM), and particularly specialist tools for three-dimensional electromagnetic simulation in both time and frequency domains on volume and surface meshes, such as the CST Microwave Studio. Particularly, this tool uses, in simulations, the perfect boundary approximation (PBA) and the thin sheet technique (TST) to increase the modeling precision in comparison with the conventional software (Chung, 2001).

The electromagnetic parameters can be deduced from the scattering parameters (De Paula et al.; ASTM, 2001; Nicolson and Ross, 1970; Weir, 1974; Agilent Technologies, 1985). For this, the boundaries of the material under test (MUT) are defined and afterwards the S parameters can be accurately known. The following equations relate the parameters S_{11} (scattering parameter related to the radiation emission from port 1 and collect in port 1) and S_{21} (scattering parameter related to the

Received: 06/11/10
Accepted: 11/11/10

radiation emission from port 1 and collect in port 2) (Fig. 1) to the reflection and transmission coefficients Γ and T , respectively. These equations allow to solve the boundary-condition problem at $\ell = 0$ (ℓ is the line of air) and $\ell = d$ (d is the sample thickness) (Fig. 1), such that the reflection coefficient can be expressed as Eq. 1 and 2 (ASTM, 2001; Nicolson and Ross, 1970):

$$\Gamma = K \pm \sqrt{k^2 - 1} \quad (1)$$

where:

$$K = \frac{\{S_{11}^2(\omega) - S_{21}^2(\omega)\} + 1}{2S_{11}(\omega)} \quad (2)$$

The transmission coefficient is given by Eq. 3:

$$T = \frac{\{S_{11}(\omega) + S_{21}(\omega)\} - \Gamma}{1 - \{S_{11}(\omega) + S_{21}(\omega)\} \Gamma} \quad (3)$$

From Eq. 1 and 3, auxiliary variables (x and y) are defined as follows (Eq. 4 to 7) (ASTM, 2001; Nicolson and Ross, 1970):

$$x = \frac{\mu_r}{\mathcal{E}_r} = \left(\frac{1 + \Gamma}{1 - \Gamma} \right)^2 \quad (4)$$

$$y = \mu_r \cdot \varepsilon_r = \left\{ \frac{c}{\omega d} \ln \left(\frac{1}{T} \right) \right\}^2 \quad (5)$$

$$\mu_r = \sqrt{x \cdot y} \quad (6)$$

$$\mathcal{E}_r = \sqrt{\frac{y}{x}} \quad (7)$$

where,

c = speed of the light in the free space;

μ_r = relative permeability of material;

\mathcal{E}_r = relative permittivity of material;

ω = angular speed.

For measurements using a rectangular waveguide sample holder, Eq. 4 and 5 can be rewritten as Eq. 8, 9 and 10 (ASTM, 2001; Nicolson and Ross, 1970):

$$\frac{1}{\Lambda^2} = \left(\frac{\mathcal{E}_r \cdot \mu_r}{\lambda_0^2} - \frac{1}{\lambda_c^2} \right) = - \left[\frac{1}{2\pi d} \ln \left(\frac{1}{T} \right) \right]^2 \quad (8)$$

$$\mu_r = \frac{1 + \Gamma}{\Lambda(1 - \Gamma) \left(\frac{1}{\lambda_0^2} - \frac{1}{\lambda_c^2} \right)} \quad (9)$$

$$\mathcal{E}_r = \frac{\left(\frac{1}{\Lambda^2} - \frac{1}{\lambda_c^2} \right) \lambda_0^2}{\mu_r} \quad (10)$$

Where,

λ_0 is the free space wavelength and λ_c the cutoff wavelength of the guide.

Since the material is a passive medium, the signal of the square root in Eq. 1 is determined by the requirement that $\text{Re}(1/\Lambda) > 0$. It is also noted that Eq. 9 and 10 can be applied for measurements using a coaxial sample holder, for which $\lambda c \rightarrow \infty$.

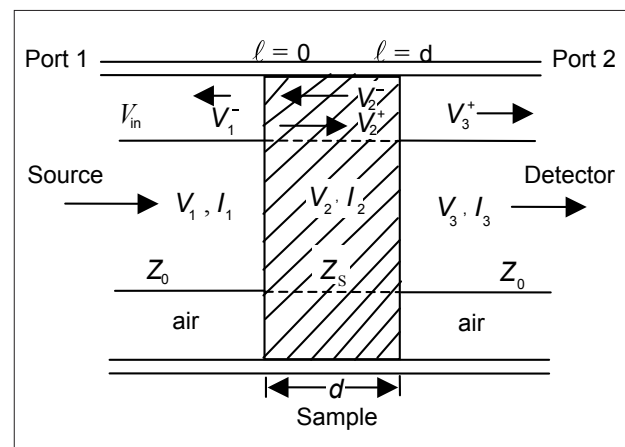


Figure 1: Waveguide filled with material. (Z_0 is the impedance of air, Z_s is the impedance of the material, V_n ($n = 1, 2, 3, \dots$) is the voltage, I_n ($n = 1, 2, 3, \dots$) is the intensity, n is the interface between the means, d is the sample thickness and ℓ is the thickness of line of air (ASTM, 2001; Nicolson and Ross, 1970).

One methodology that makes use of the scattering parameters S_{11} and S_{21} to calculate the mentioned complex parameters of samples is named Nicolson-Ross-Weir (NRW) (Nicolson and Ross, 1970; Weir, 1974). The NRW modeling is the most common used method to perform the calculation of complex permittivity and permeability of materials. This modeling has the advantage of being non-interactive (no interactive procedure is needed), as required in the Baker-Jarvis method (Baker-Jarvis et al., 1993). Besides this, the NRW modeling is applicable for coaxial line and rectangular waveguide cells. On the other side, it is known that the NRW can diverge for low-loss materials at frequencies corresponding to integer multiples of one half wavelength in the sample (Nicolson and Ross, 1970; Weir, 1974). At this particular frequency, the magnitude of the measured S_{11} parameter is particularly smaller (thickness resonance) and the S_{11} phase uncertainty becomes larger. This behavior can lead to the appearance of inaccuracy peaks on the permittivity and permeability curves.

Considering the knowledge importance on the complex permittivity and permeability of materials aiming the adequate characterization of them and new developments, the present work presents a study involving measured and simulated complex permittivity and permeability of a Teflon® (polydifluoroethylene) test sample with 11.75 mm thick. Herein, the experimental complex parameters were retrieved using the NRW modeling. Simulated frequency-dependent quantities were obtained by CST tool and these results are compared with experimentally measured values in the 8.2-12.4 GHz frequency range (X-band).

MATERIALS AND METHODS

Experimental Measurements

In this study, the experimental methodology was performed according to the steps depicted in Fig. 2. For this, it was assembled a setup including an automatic vector network analyzer (VNA) HP8510C, which was connected as a source and measurement equipment. During calibration, standard setup values must be stored, so that when making calibration, the measured and reference values are compared to characterize measurement systematic errors (ASTM, 2001). The calibration also establishes the reference planes for the measurement test ports. Figure 3 shows the calibration X band kit used in this paper.

To determine the complex permittivity and permeability, via S-parameters (S_{11} and S_{21}), it was used the two-port transmission/reflection approach, with a material-under-test (Teflon® sample with 11.75 mm thick) of smooth flat faces, and filling completely the fixture cross section, being placed inside a rectangular waveguide (Fig. 4). The

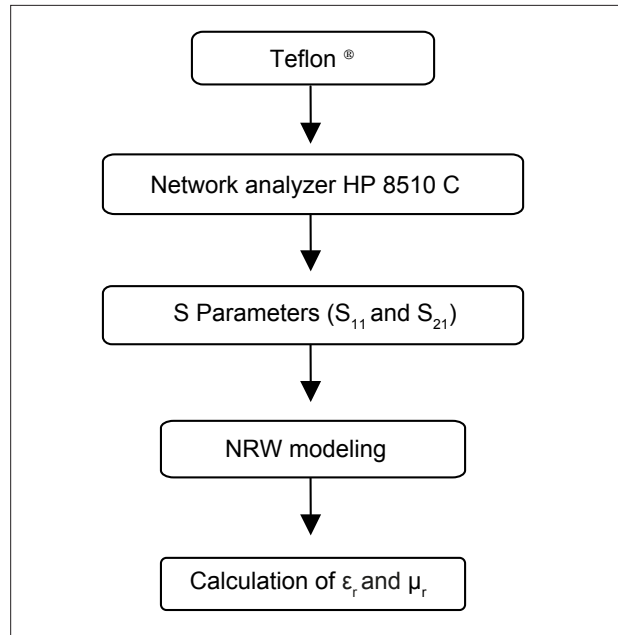


Figure 2: Flow chart of complex permittivity and permeability experimental measurements.



Figure 3: Waveguide calibration set for X band.

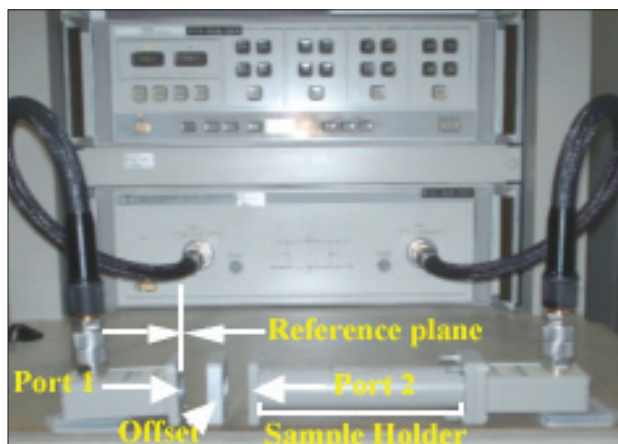


Figure 4: Setup for measurements of S-parameters.

sample holder is a precision waveguide section of 140 mm length, which is provided with the calibration kit. When measuring the scattering parameters, the offset, placed between ports 1 and 2, is closed with the sample holder. The adapter of port 1 is taken as the reference plane (Fig. 4).

After the S-parameters measurements, the complex parameters (ϵ^* and μ^*) were calculated according to the NRW modeling, as depicted in Fig. 2.

Numerical Simulations

The numerical simulations were carried out according to flow chart presented in Fig. 5. In this case, the electromagnetic parameters were deduced from a scattering matrix defined between the sample planes (marked in red), as shown in Fig. 6. The used complex parameters for the

Teflon[®] sample were based on the literature ($\epsilon_r = 2.04-0.0j$ and $\mu_r = 1.0-0.0j$) (ASTM, 2001).

Based on the complex parameters from literature (ASTM, 2001) and on the scattering matrix defined in this study (Fig. 6), the MS-CST tool was used to simulate the scattering parameters S_{11} and S_{21} of the Teflon[®] sample. Afterwards, from the magnitude and phase values of the simulated parameters, the complex parameters were retrieved according to Fig. 5.

RESULTS AND DISCUSSION

Measured and calculated scattering parameters of a Teflon[®] test sample with thickness of 11.75 mm are compared in Figs. 7 and 8. In Fig. 7, the experimental and numerical S_{21} parameters both coincide and they are near 0 dB level in magnitude. Experimental and numerical S_{21} parameters related to the inversion of phase also show

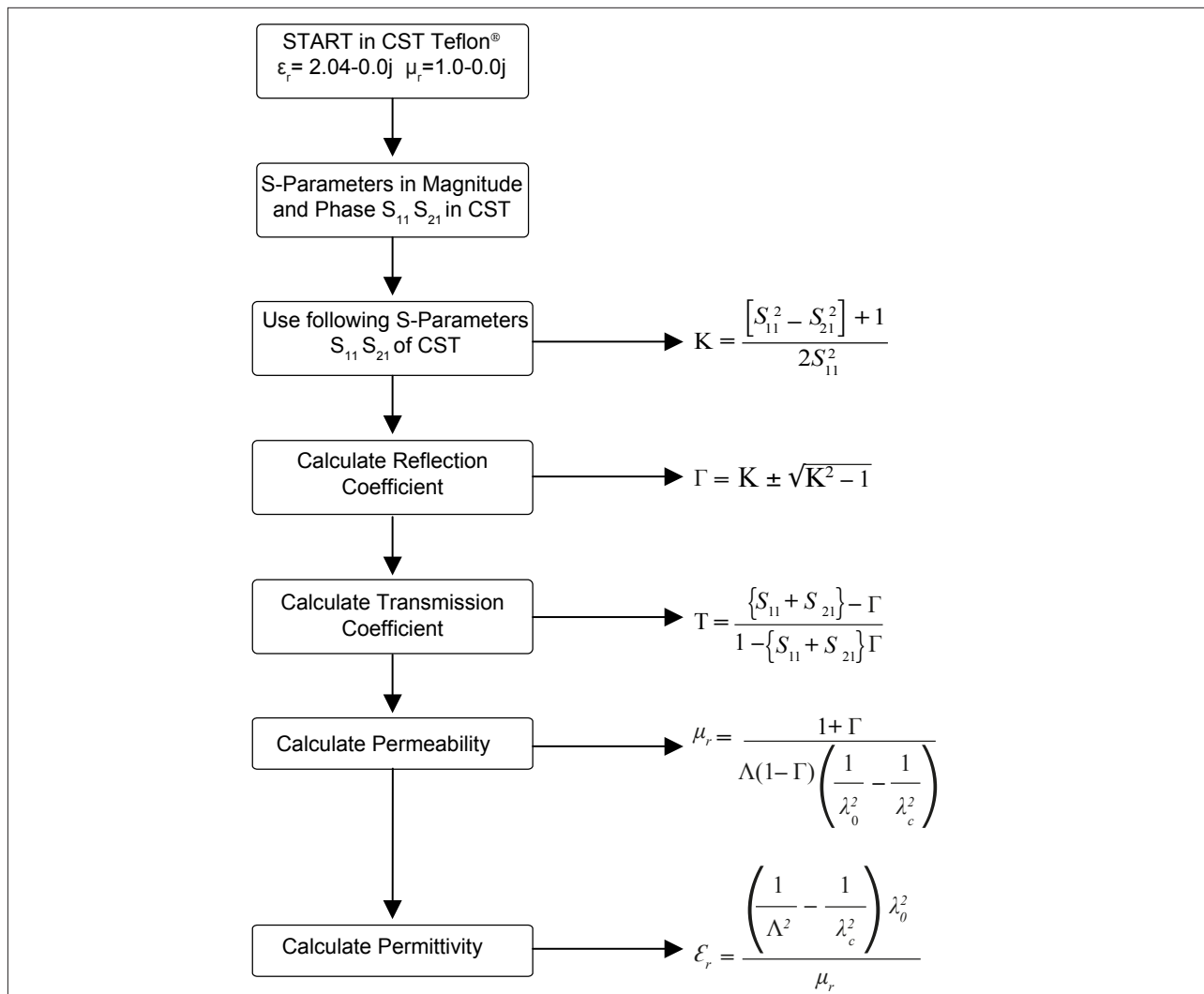


Figure 5: Flow chart of the numerical simulation used in the complex permittivity and permeability calculation.

a good agreement (Fig. 8). The scattering parameter S_{11} (experimental and numerical) shows a resonance at the 10.04 GHz frequency (Fig. 7), but it is also observed a slight difference in the maximum amplitude value, in which the simulated S_{11} resonance presents a higher attenuation value (~ 55 dB) than the experimental one (~ 45 dB). To understand this difference is important to mention that the simulation configuration depicted in Fig. 6 takes place in an ideal environment, where temperature, humidity, misalignment, and air gap effects are not taken into account.

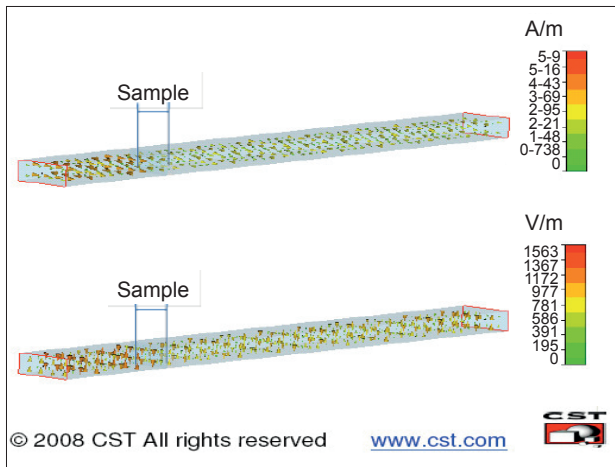


Figure 6: Configuration modeling of electric and magnetic fields in X band rectangular waveguide. Sample planes are marked in red line. In the scale: red means a greater interaction of the electrical (A/m scale) and magnetic (V/m scale) fields with the sample (material), and green means a lower wave-sample interaction.

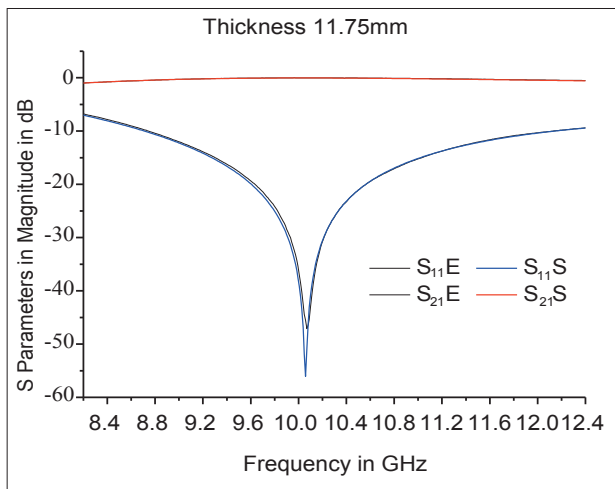


Figure 7: Experimental and simulated parameters of S_{11} and S_{21} in magnitude of Teflon[®] with 11.75 mm thickness (E - experimental and S - simulated).

A careful analysis of Fig. 8 shows that measured and simulated S_{11} curves in phase present any difference, where the simulated S_{11} curve bends downward in the frequency range of ~ 10.1 to ~ 10.7 GHz. This behavior is attributed to the actual interaction of the electromagnetic wave with the material in phase (Fig. 8), considering that the simulation takes place in an ideal environment, as already mentioned.

Then, based on the NRW procedure, the S-parameters were used to determine ϵ^* and μ^* , which are given in Figs. 9 and 10, respectively. In a general way, these figures show that the agreement between measured and simulated quantities is quite satisfactory, except for the calculated ϵ' . These results allow to infer that the bending effect on

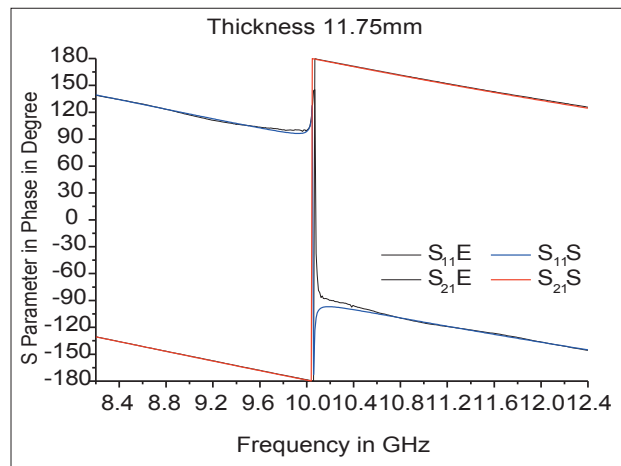


Figure 8: Experimental and simulated parameters of S_{11} and S_{21} in phase of Teflon[®] with 11.75 mm thickness (E - experimental and S - simulated).

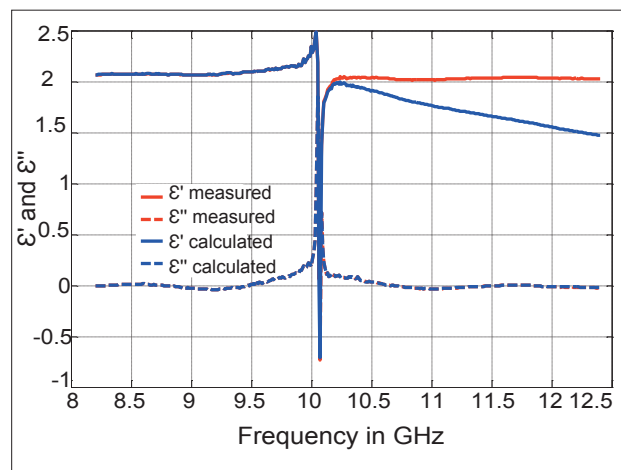


Figure 9: Test sample complex permittivity $\epsilon^* = \epsilon' - j\epsilon''$: measured (red curves) and calculated (blue curves) using the NRW modeling.

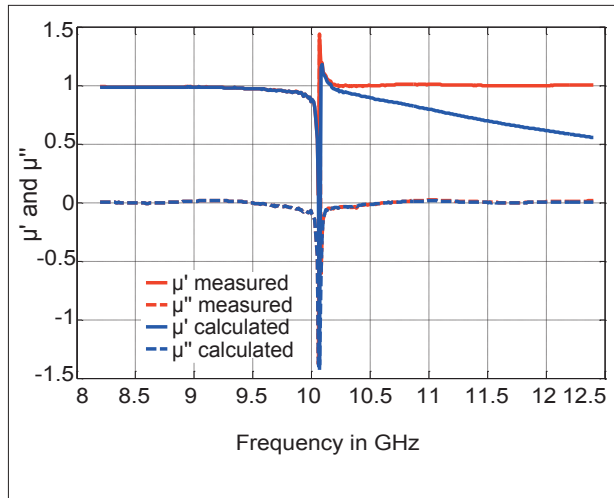


Figure 10: Test sample complex permeability $\mu^* = \mu' - j\mu''$: measured (red curves) and calculated (blue curves) using the NRW modeling.

the simulated S_{11} curve, which was observed in Fig. 8 (in the frequency range of $\sim 10.1 - 10.7$ GHz), is translated into a decrease of ϵ' and μ' at higher frequencies (Figs. 9 and 10).

CONCLUSION

The comparative study of the electromagnetic parameters of a Teflon® slab shows a good agreement between measured and simulated complex permittivity and permeability, which were retrieved using the NRW modeling. From these results, it is possible to conclude that the used procedure guarantees an accuracy experimental characterization of materials and their simulation. It was also noted that the tested procedure proved to be robust, and no anomalies were noticed because resonance for the 11.75-mm-thickness sample occurs above 10.04 GHz. This result overcomes a possible disadvantage of using the NRW modeling, as previously mentioned in this text.

ACKNOWLEDGMENTS

The authors are thankful to the Aerospace Technology and Science Department (DCTA, acronym in Portuguese), Institute of Aeronautics and Space, Financiadora de Estudos e Projetos – FINEP (Project No. 1757/03) and

CNPq (Project no. 305478/2009-5) for the financial supports.

REFERENCES

Agilent Technologies, “Measuring the dielectric constant of solids with the HP 8510 network analyzer”, Technical Overview 5954-1535.USA, 10p., 1985.

American Society for Testing and Materials, “ASTM D5568-1: Standard Test Method for measuring Relative Complex permittivity and Relative Magnetic Permeability of Solid Materials at Microwave Frequencies”, West Conshohocken, PA: ASTM, 2001.

Baker-Jarvis, J., Janezic, M. D., Grasvenor Jr., J. H., and Geyer, R. G., “Transmission/Reflection and Short-Circuit Line of Methods for Measuring Permittivity and Permeability”, NIST Technical Note 1355-R, Colorado, 1993, from http://whites.sdsmt.edu/classes/ee692gwmm/additional/NIST_Tech_Note_1355-R.pdf.

Chung, B. K., “Dielectric constant measurement for thin material at microwave frequency”, Progress in Electromagnetics Research, Vol., No. 75, pp. 239-252, 2007.

CST MICROWAVE STUDIO. Version 3 Getting Started, Jan.2001, CST Computer B.-K Chung, “Dielectric constant measurement for thin material at microwave Simulation Technology”.

De Paula, A. L., Rezende, M. C., Barroso, J. J., Pereira, J. J. and Nohara E. L., “Comparative Study of S parameters of the Teflon® obtained experimentally and by Electromagnetic Simulation”, Symposium on Operating Systems Application Areas of Defense, São José dos Campos, Brazil, 2008.

Nicolson, A. M., Ross, G. F., “Measurement of the Intrinsic Properties of Materials by Time Domain Techniques”, Instrumentation and Measurement, Vol. 19, pp.377-382, 1970. doi: 10.1109/TIM.1970.4313932

Weir, W.B., “Automatic Measurement of Complex Dielectric Constant and Permeability at Microwave Frequencies”, Proceedings of the IEEE, Vol. 62, pp. 33-36, 1974.